2014 IEEE International Conference on Robotics & Automation (ICRA)
Hong Kong Convention and Exhibition Center
May 31 - June 7, 2014. Hong Kong, China

Tipover Stability Enhancement Method for A Tracked Mobile Manipulator

Huatao Zhang and Aiguo Song

Abstract— **The system center of gravity (SCG) is a critical element for the stability of a robot when it undergoes locomotion. In this paper, we propose a new algorithm for enhancing such stability by manipulating the location of the SCG. Specifically, we can prevent the robot from tipping over, rolling over, and tumbling over. The tipover stability criteria for a tracked mobile manipulator are discussed and the velocity kinematic model of the manipulator for SCG adjustment is also presented in this paper. The embedded 3-axial gyroscope provides us the data necessary for the SCG computation. The algorithm outputs the adjustments needed on the joint angles in order to maintain the SCG within a body-fixed safety zone. The experimental results verified the effectiveness of the proposed algorithm.**

I. INTRODUCTION

Despite having the dual advantages of mobility and dexterity, mobile manipulator is often trading its stability and reliability for advantages. However, mobile manipulators are usually designed for tough work in hazardous environments. They always need to maneuver through difficult terrain. Such environments are especially dangerous and challenging for the mobile manipulators.

Nowadays, many researchers have been making and designing the mobile manipulator for wide variety of applications. A lot of efforts have been made in order to allow the mobile robot to adapt to the complex environment. Depending on the type of locomotion, mobile robots can be categorized as legged robots, wheeled robots, tracked robots and hybrid robots. With the development of reconfigurable robots, many researches focus on the mechanical structure design for the robot system to enhance the obstacle crossing performance. Raibert et al. [1] developed the famous rough-terrain quadruped robot (Bigdog). Moore et al.[2] proposed a reliable stair climbing method for the hexapod RHex to climb up the full-size stairs. Woo et al.[3] designed a new wheeled robot with a passive linkage-type locomotion structure to achieve the obstacle crossing purpose. In related researches with tracked mobile robots, the all-terrain mobile robot iRobot Packbot [4] was developed for military applications, and Matthies and Xiong et al. [5] developed the urban robot Urbie based on the Packbot structure. Some autonomous stair climbing algorithms for tracked robots are proposed and applied to Packbot and Urbie [6], [7].

While the obstacle crossing ability of the mobile robot has been extensively studied, only a few researches have been reported on the tipover stability. Mosadeghzad et al. [8] proposed a method to change the structure of the reconfigurable robot so as to decrease the probability of tipping over on rocky terrain. Ghaffari et al. [9] developed an adaptive neuro-fuzzy inference controller to enhance the tipover stability for a nonholonomic mobile manipulator. Even less work has been reported on the tipover stability enhancement for the tracked mobile robot as it climbs stairs or crosses obstacles. Liu [10] analyzed the interaction between the track and stairs and proposed tipover prevention algorithm for a tracked mobile manipulator. However, the algorithm just stops the robot before tipover occurs, rather than improving the tipover stability. In our previous work [11], the relationship between stairs climbing ability and centroid position is presented, but still remains in a tipover stability analysis stage.

In this paper, we focus on the enhancement of the system center of gravity (SCG) based tipover stability for a tracked search and rescue robot (SRR) which was developed in our laboratory. This SRR is a nonholonomic mobile manipulator consisting of a 4-DOF manipulator and a tracked mobile base, also a 3-axial gyroscope is mounted for gathering the orientation data of the robot. For the organization of the rest of this paper, we first present the kinematic model of the SRR and the SCG distribution area. Secondly, the SCG based tipover criteria for the SRR are discussed. Then, the velocity kinematic model of manipulator for SCG adjustment is presented. As for the solution section, this paper proposes a new tipover avoidance method for the SRR by using the manipulator adjustment. In addition, a redundancy resolution method which was introduced in our previous work [12] is also employed in this algorithm. Finally, we present and discuss about our experimental results.

II. SYSTEM MODELING

The robot presented in Fig.1 is an improved prototype of our search and rescue robot [11] with the ability of crossing obstacles. Fig.2 shows the different robot coordinate systems. Because the last joint does not affect the SCG, we simplify the 4-DOF manipulator as a 3-DOF manipulator in this paper.

The XYZ frame is the local fixed tangent plane coordinate system. The angles r, p, β are typical roll, pitch, yaw. The coordinate systems $X_pY_pZ_p$, $X_tY_tZ_t$ and $X_bY_bZ_b$ coordinate system are all located at the center of gravity of mobile base (marked as *mb* in Fig.2). The $X_pY_pZ_p$ frame is platform coordinate system, the axes direction are the same as XYZ frame. The $X_bY_bZ_b$ frame is the mobile base coordinate system. The $X_tY_tZ_t$ frame is tipover estimation coordinate system, it can be obtained by rotating the $X_pY_pZ_p$ frame through β

This work was supported by the National Natural Science Foundation of China No.61272379 and 61325018

Huatao Zhang and Aiguo Song are with School of Instrument Science and Engineering, Southeast University, Nanjing, 210096, China. (h.t.zhang@seu.edu.cn; a.g.song@seu.edu.cn)

Fig. 1. Tracked search and rescue robot

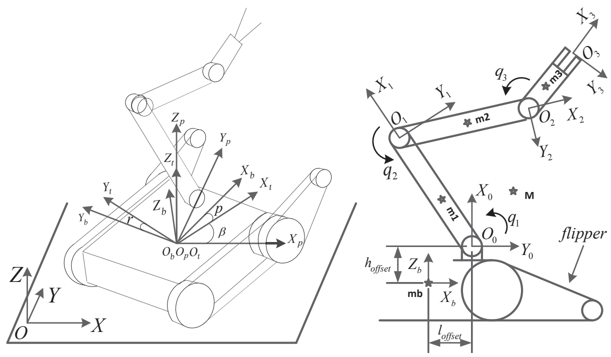

Fig. 2. Coordinate system of SRR

angle related to Zp direction. $X_0Y_0Z_0$ coordinate system is situated at the junction of mobile base and manipulator. The transformation matrix among these coordinate systems are expressed as

$$\begin{aligned} B_t^p =& Rot_{Z,\beta} \\ B_b^t =& Rot_{Y,p} Rot_{X,r} \\ B_0^b =& Trans_{X,l_{offset}} Trans_{Y,w_{offset}} Trans_{Z,h_{offset}} \\ & \cdot Rot_{X,-90^\circ} Rot_{Z,-90^\circ} \end{aligned} \tag{1}$$

Table I shows the Denavit-Hartenberg variables and parameters of the manipulator. The general transformation matrix of the manipulator is expressed as

$$A_i^{i-1} = \begin{bmatrix} Cq_i & -Sq_i & 0 & a_iCq_i \\ Sq_i & Cq_i & 0 & a_iSq_i \\ 0 & 0 & 1 & d_i \\ 0 & 0 & 0 & 1 \end{bmatrix} \tag{2}$$

where index i denotes the i-th link of the manipulator, and C and S denote cosine and sine respectively.

TABLE I
DENAVIT-HARTENBERG VARIABLES AND PARAMETERS

i	$a_i(mm)$	$d_i(mm)$	$\alpha_i(^\circ)$	$\theta_i(^\circ)$
1	l_1	0	0	q_1
2	l_2	-s	0	q_2
3	l_3	0	0	q_3

The forward kinematics of this SRR can be obtained according to these transformation matrices. The location of the SCG of the whole robot system can also be derived from the forward kinematics.

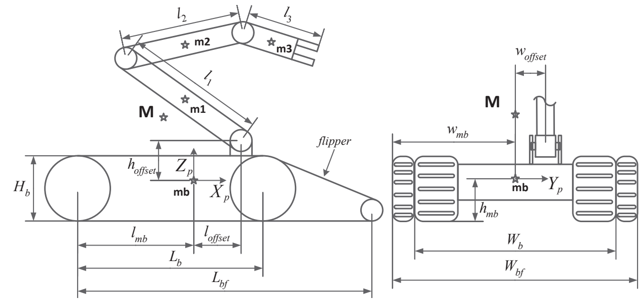

Fig. 3. Distribution of the center of gravity and dimensional parameters of SRR

The distribution of the center of gravity and dimensional parameters of this SRR are shown in Fig.3. Because of the relative light weight and small movement of the flipper, we ignored the contribution of the flipper in the SCG calculation. Therefore, for the mobile base, the location of the center of gravity is a fixed point. The center of gravity of each individual manipulator link is located at the center point. The position of SCG can be calculated as

$$\xi_M = \frac{\sum_{i=1}^{3} m_i \xi_{mi}}{\sum_{i=1}^{3} m_i + m_b} = \frac{\sum_{i=1}^{3} m_i \xi_{mi}}{M} \tag{3}$$

where m_i is the mass of i-th link, m_b is the mass of mobile base, ξ_{mi} is the center of gravity position of i-th link, M is the mass of whole system.

Due to the mechanical limitation, the reachable space of the manipulator is actually a 2D fan in $X_bO_bZ_b$ plane. Thus, the possible location of the SCG also lies in a 2D fan in $X_bO_bZ_b$ plane. In addition, for the purpose of protecting the manipulator, the motion space of each manipulator joint is limited above the $X_0O_0Z_0$ plane. Then, the entire area of the possible location of the SCG can be calculated by using forward kinematics and Eq.3, it is a fan shape, a sub region of the reachable space of the manipulator in $X_bO_bZ_b$ plane as shown in Fig.4.

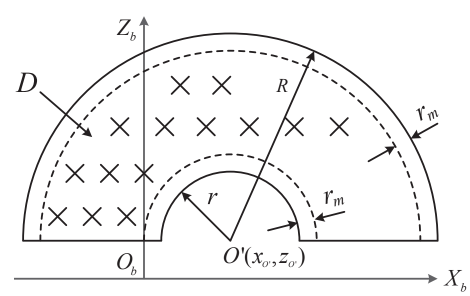

Fig. 4. The area of the possible location of the SCG

A positive margin r_m is added in order to avoid the singular posture for the manipulator in Fig.4. The area of the possible location of the SCG D could be expressed analytically as

$$D = \begin{cases} z_m \geq z_{o'} \\ (x_m - x_{o'})^2 + (z_m - z_{o'})^2 \leq (R - r_m)^2 \\ (x_m - x_{o'})^2 + (z_m - z_{o'})^2 \geq (r + r_m)^2 \end{cases} \tag{4}$$

where

$$\begin{cases} x_{o'} = \dfrac{m_1 + m_2 + m_3}{M} l_{offset} \\ z_{o'} = \dfrac{m_1 + m_2 + m_3}{M} h_{offset} \\ R = \dfrac{\frac{l_1}{2} m_1 + (l_1 + \frac{l_2}{2}) m_2 + (l_1 + l_2 + \frac{l_3}{2}) m_3}{M} \\ r = \dfrac{\frac{l_1}{2} m_1 + (l_1 - \frac{l_2}{2}) m_2 + (l_1 - l_2 - \frac{l_3}{2}) m_3}{M} \end{cases} \tag{5}$$

The SCG can move around within the area D as the manipulator changes its posture. Hence, we have a tactic to improve the tipping stability if we can relate SCG to the tipover stability.

III. TIPOVER STABILITY ANALYSIS

The SRR tipover could be generally divided into three categories: rollover, backward tipover and forward tipover. In this paper, we focus on the first two situations because the third one is relatively simple.

A. Rollover stability analysis

Rollover usually occurs when the SRR traversing through obstacles with only single track or moving laterally on a slope.

First, the simple case only with roll angle r is analyzed. The rollover safety zone and rollover critical state are shown in Fig.5.

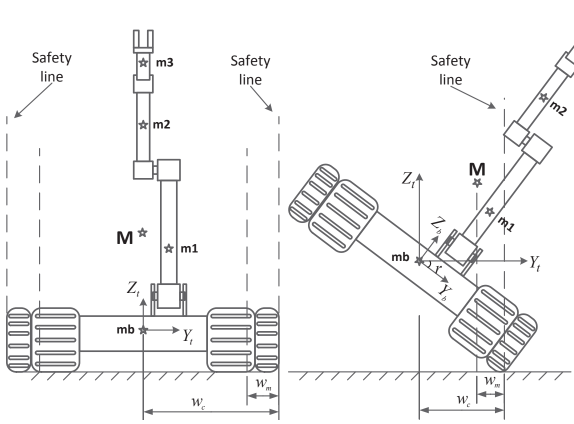

Fig. 5. Rollover safety zone and critical state of SRR

The variable w_c is defined as a safety distance as shown in Fig.5, it is calculated as

$$w_c = |w_{mb} \cos r| - |h_{mb} \sin r| \tag{6}$$

where r is roll angle, w_{mb} and h_{mb} are as defined in Fig.3.

The rollover safety zone is located between the two safety lines. The robot system is safe when SCG in the rollover safety zone. Otherwise, the system will rollover. In addition, we add a margin w_m to ensure a safety factor for the robot system. Thus, the safety criterion of SRR system in this case could be described as

$$\left| y_M^t \right| \leq w_c - w_m \tag{7}$$

where y_M^t is Y_t-axis coordinate of SCG.

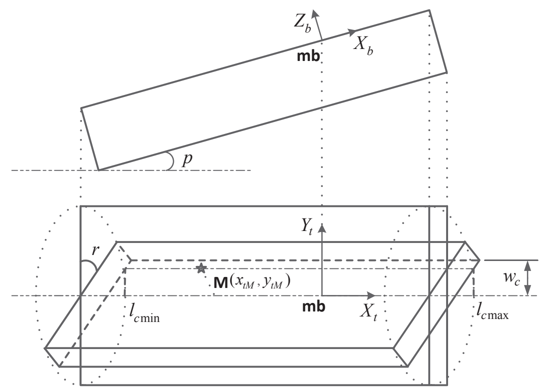

Fig. 6. Simplified posture of SRR with roll angle r and pitch angle p

Secondly, we are going to analyze the general case which contains roll angle r and pitch angle p. The simplified posture of SRR is shown in Fig.6. we can easily conclude that the pitch angle does not affect the Y_t-axis coordinate of SCG. Therefore, the safety criterion described by Eq.6 and Eq.7 still remains valid. However, the pitch angle will lead to the changes in X_t-axis coordinate of SCG. According to the geometric relationship and the coordinate transformation analysis, the safety range for X_t-axis coordinate of SCG can be expressed as

$$\begin{cases} x_M^t \leq l_{cmax} = k y_M^t + b_1 - l_m \\ x_M^t \geq l_{cmin} = k y_M^t + b_2 + l_m \end{cases} \tag{8}$$

where x_M^t is X_t-axis coordinate of SCG. l_m is also a margin distance. k, b_1 and b_2 are calculated as

$$\begin{cases} k = \dfrac{\sin r \sin p}{\cos r} \\ b_1 = (l_{bf} - l_{mb}) \cos p - \dfrac{h_{mb} \sin p}{\cos r} \\ b_2 = (-l_{mb}) \cos p - \dfrac{h_{mb} \sin p}{\cos r} \end{cases} \tag{9}$$

B. Backward tipover stability analysis

Backward tipover stability is also closely related to the SCG. Stair is a typical obstacle for SRR to deal with in the building. The backward tipover stability analysis for the SRR climbing stairs is presented in this section. Fig.7 is an illustration of the SRR climbing a stair. The height and depth of the stair are denoted as h_{step} and d_{step} respectively. θ_s denotes the stairs angle; e_c represents the distance between the gravity line of SCG M and the touch point C on the stair edge. l_M indicates the distance between M and the tail of SRR. h_M indicates the height of M from the SRR bottom plane.

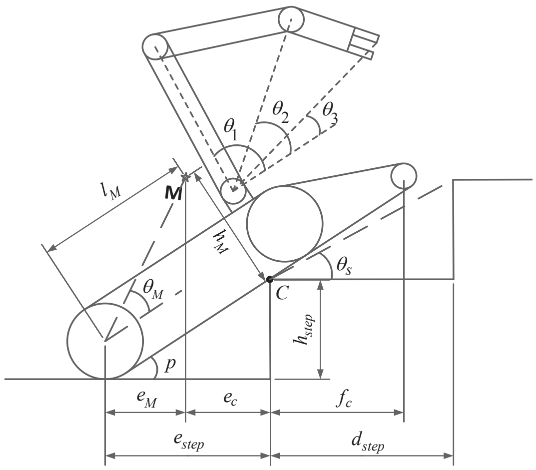

Fig. 7. SRR climbing staris

In the process of stairs climbing, the SRR will succeed to climb onto the stairs if the gravity line of SCG reach or pass the touch point C, which means $e_c \leq 0$. Otherwise, the SCG will move backward and SRR will fail to climb the stairs. e_c is calculated as

$$e_c(p, l_M, h_M) = \frac{h_{step}}{\tan p} - (l_M \cos p - (h_M - r_w) \sin p) \tag{10}$$

where r_w is the radius of the rear wheel.

Assuming that the rear wheels of SRR always touching the ground, the pitch angle p of SRR will keep increasing during stairs climbing. There exists a unique pitch angle $p \in [0, \pi/2]$ that minimizes e_c.

$$\left.\frac{\partial e_c}{\partial p}\right|_{p\in[0,\pi/2]} = l_M \sin p + (h_M - r_w) \cos p - h_{step}(1 + \cot^2 p) = 0 \tag{11}$$

The solution for p in eq.11 is denoted as p_m, and the minimum e_c is expressed as

$$e_{cmin} = e_c(p_m, l_M, h_M) \tag{12}$$

The safety criterion for SRR to climb onto the stairs is described as

$$e_{cmin} \leq -e_m \tag{13}$$

where e_m is a positive margin to enhance the safety for SRR.

Beside knowing whether the SRR is safe to climb a stair, we also want to figure out how to adjust the SCG to improve the stability and the ability for the SRR climbing stairs. If e_{cmin} satisfies Eq.13, there must be at least one solution for p in equation: $e_c(p) = 0$, the minimum solution is denoted as p_f. When pitch angle reaches p_f, the robot system will turn forward to climb onto the stair. For stairs with known height, it can be concluded that the longer the length l_M is, and the lower the height h_M is, the smaller the angle p_f will be. However, considering the smoothness for SRR climbing stairs, we will not choose the smallest p_f as the desired angle of turning forward. The desired angle is selected as

$$p_d = k_p \theta_s = k_p \arctan(\frac{h_{step}}{d_{step}}) \tag{14}$$

where k_p is a scale factor, and is usually slightly less than 1.

It is easy to understand that the SRR produces minimum vibration in stairs climbing process when the forward turning angle is equal to the stairs angle. Therefore, we only need to find out appropriate SCG (l_M and h_M) to satisfy $p_f = p_d$.

IV. TIPOVER AVOIDANCE METHOD BASED ON MANIPULATOR ADJUSTMENT

The algorithm for SRR tipover avoidance is presented in this section. It is proposed to adjust the SCG by changing the configuration of manipulator.

Let the configuration vector be $q = [q_1\ q_2\ q_3]^T$, where $q_i (i = 1, 2, 3)$ is the ith joint angle of the manipulator. Set $\xi_{mi} = [x_{mi}\ y_{mi}\ z_{mi}]^T$, where ξ_{mi} is the center of gravity position of the i-th link in $X_pY_pZ_p$ frame. The velocity vector of ξ_{mi} is given as

$$\begin{aligned}
\dot{\xi}_{m1} &= [Z_0 \times \overrightarrow{O_0O_{m1}}\ \ 0\ \ 0]\dot{q} = J_{m1}\dot{q} \\
\dot{\xi}_{m2} &= [Z_0 \times \overrightarrow{O_0O_{m2}}\ \ Z_1 \times \overrightarrow{O_1O_{m2}}\ \ 0]\dot{q} = J_{m2}\dot{q} \\
\dot{\xi}_{m3} &= [Z_0 \times \overrightarrow{O_0O_{m3}}\ \ Z_1 \times \overrightarrow{O_1O_{m3}}\ \ Z_2 \times \overrightarrow{O_2O_{m3}}]\dot{q} = J_{m3}\dot{q}
\end{aligned} \tag{15}$$

where Z_i is the Z-axis of the (i+1)-th joint coordinate frame, $\overrightarrow{O_iO_{mj}}$ is a vector from the (i+1)-th joint to the center of gravity of j-th link in $X_pY_pZ_p$ frame, J_{mi} is the Jacobian of i-th link center of gravity.

However, considering the mechanical structure of our SRR, The reachable space of link center of gravity and SCG is limited in $X_bO_bZ_b$ plane as mentioned in section II. Therefore, the center of gravity position of the i-th link can be expressed as $\xi^b_{mi} = [x^b_{mi}\ z^b_{mi}]^T$, and the Jacobian of link center of gravity is changed as

$$\begin{aligned}
J^b_{m1} &= [\ {}^{\perp}\overrightarrow{O^b_0O^b_{m1}}\quad 0\quad 0\ ] \\
J^b_{m2} &= [\ {}^{\perp}\overrightarrow{O^b_0O^b_{m2}}\quad {}^{\perp}\overrightarrow{O^b_1O^b_{m2}}\quad 0\ ] \\
J^b_{m3} &= [\ {}^{\perp}\overrightarrow{O^b_0O^b_{m3}}\quad {}^{\perp}\overrightarrow{O^b_1O^b_{m3}}\quad {}^{\perp}\overrightarrow{O^b_2O^b_{m3}}\ ]
\end{aligned} \tag{16}$$

where $\overrightarrow{O^b_iO^b_{mj}}$ is a vector from the (i+1)-th joint to the center of gravity of j-th link in $X_bY_bZ_b$ frame, ${}^{\perp}\overrightarrow{O^b_iO^b_{mj}}$ is a vector perpendicular to $\overrightarrow{O^b_iO^b_{mj}}$, and

$$if\ \overrightarrow{O^b_iO^b_{mj}} = [x^b_{ij}\ \ z^b_{ij}]^T,\ then\ {}^{\perp}\overrightarrow{O^b_iO^b_{mj}} = [z^b_{ij}\ \ -x^b_{ij}]^T$$

The desired task velocity vector of SCG is obtained as

$$\dot{\xi}^b_M = \frac{\sum_{i=1}^{3} m_i \dot{\xi}^b_{mi}}{M} = \frac{\sum_{i=1}^{3} m_i J^b_{mi}}{M}\dot{q} = J^b_M \dot{q} \tag{17}$$

where $\xi_M^b \in \Re^2$ is the SCG in $X_bO_bZ_b$ plane, J_M^b is the Jacobian of SCG.

Since $q \in \Re^3$ and $\xi_M^b \in \Re^2$, the robot system is redundant. Some redundancy resolution schemes is introduced in our previous work [12]. For given task $\dot{\xi}_M^b$, all solutions q to the velocity kinematics in Eq. 17 can be expressed as

$$\dot{q} = J_M^{b\dagger}\dot{\xi}_M^b + (I - J_M^{b\dagger}J_M^b)q_s \tag{18}$$

where the $J_M^{b\dagger}$ is the right pseudo inverse of matrix J_M^b, $I - J_M^{b\dagger}J_M^b$ is the null-space of J_n, and $q_s \in \Re^3$ is an arbitrary vector. It consists of some secondary tasks which will affect the internal structure of manipulator without affecting the final control of the main task.

In this paper, we simply choose the joint limit avoidance and singularity removing functions to enhance the safety and stability of SRR. These functions are also mentioned in [12], expressed as

$$\begin{cases} H_1 = (-\frac{1}{2})\sum_{i=1}^{3}(\frac{1}{q_i - q_{\min i}})^2 + (\frac{1}{q_i - q_{\max i}})^2 \\ H_2 = \sqrt{\det(J_M^b \cdot (J_M^b)^T)} \end{cases} \tag{19}$$

where $q_{\min i}$ and $q_{\max i}$ are the minimum limiting angle and the maximum limiting angle respectively for each i-th joint.

Based on the prior stability criteria and velocity kinematics for SCG, the Alg.1 illustrates the rollover avoidance algorithm. On the other hand, the Alg.2 illustrates the backward tipover avoidance algorithm for SRR climbing stairs.

Algorithm 1 Rollover avoidance

repeat
  $\xi_M \leftarrow f(\beta, p, r, q_1, q_2, q_3)$
  $\xi_M^t \leftarrow (B_t^p)^T \xi_M$, ${}^{tmp}\xi_M^b \leftarrow (B_b^t)^T \xi_M^t$
  if $|y_M^t| > w_c - w_m$ **then**
    $y_M^t \leftarrow \mathrm{sgn}(y_M^t)(w_c - w_m)$
  end if
  if $x_M^t < l_{c\min}$ **or** $x_M^t > l_{c\max}$ **then**
    $x_M^t \leftarrow l_{c\min}$ **or** $x_M^t \leftarrow l_{c\max}$
  end if
  $\xi_M^b \leftarrow (B_b^t)^T \xi_M^t$
  if $\xi_M^b \notin D$ **then**
    find $\hat{\xi}_M^b \in D$ to minimize $((x_M^b - \hat{x}_M^b)^2 + (z_M^b - \hat{z}_M^b)^2)$
    $\xi_M^b \leftarrow \hat{\xi}_M^b$
  end if
  $[\dot{q}_1\ \dot{q}_2\ \dot{q}_3]^T \leftarrow J_M^{b\dagger}(\xi_M^b - {}^{tmp}\xi_M^b)^T + (I - J_M^{b\dagger}J_M^b)q_s$
until function stopped

In the rollover avoidance algorithm, the SCG position is calculated at first. Based on the Eq.7 and Eq.8, the algorithm also determines if any stabilizing intervention is needed. If so, the algorithm computes the desired joint velocity by using Eq.18, and activates the manipulator.

In the backward tipover avoidance algorithm for SRR climbing stairs, in step 1, the maximum length l_M and minimum height h_M is used in Eq.11 to calculate e_{cmin},

Algorithm 2 Tipover avoidance for SRR climbing stairs

solve $\dfrac{\partial e_c(l_{M\max}, h_{M\min}, p)}{\partial p} = 0$ to find p_m
$e_{c\min} \leftarrow e_c(p_m, l_{M\max}, h_{M\min})$
if $e_{c\min} > -e_m$ **then**
  Mission Aborted
end if
$\theta_s \leftarrow \arctan(h_{step}/d_{step})$, $p_d \leftarrow k_p\theta_s$
solve $e_c(p_d, l_M, h_M) = 0$ subject to Eq.4 to find ξ_M^b
if no solution for ξ_M^b **then**
  find $\xi_M^b \in D$ to minimize the distance to line $e_c(l_M, h_{M,}p_d) = 0$
end if
while $p < \arcsin(h_{step}/L_b)$ **do**
  call algorithm 1
end while
$[\dot{q}_1\ \dot{q}_2\ \dot{q}_3]^T \leftarrow J_M^{b\dagger}(\xi_M^b - {}^{tmp}\xi_M^b)^T + (I - J_M^{b\dagger}J_M^b)q_s$
$[q_1\ q_2\ q_3]^T \leftarrow [{}^{tmp}q_1\ {}^{tmp}q_2\ {}^{tmp}q_3]^T + [\dot{q}_1\ \dot{q}_2\ \dot{q}_3]^T$
for $i = 1 \rightarrow 3$ **do**
  while $p + \theta_i < \theta_s$ **do**
    call algorithm 1
  end while
end for
call algorithm 1

then the safety state of SRR is checked by using Eq.13. The algorithm will stop the stairs climbing process if Eq.13 is not satisfied. The desired forward turning angle p_d is calculated and utilized to find the desired position of SCG in step 2. The joints and end-effector of manipulator are always located in front of SRR system when the SCG reached the desired position. Collision between manipulator and stairs may occurs if the manipulator is reconfigured before the stairs climbing process. Therefore, in step 3, the algorithm will delay the manipulator reconfiguration when pitch angle p satisfies Eq.20.

$$p \geq \arcsin(\frac{h_{step}}{L_b}) \tag{20}$$

In step 4, the desired joint velocity is calculated by using Eq.18. If Eq.21 is satisfied as well, the algorithm enables the manipulator to make adjustment on the joint velocity.

$$p + \theta_i \geq \theta_s \tag{21}$$

where $\theta_i (i = 1, 2, 3)$ is as shown in Fig.7. It is also used to avoid the collision between manipulator and stairs.

Algorithm 1 is also employed in order to prevent the rollover situation caused by unexpected circumstances.

V. EXPERIMENTS

To verify the tipover avoidance algorithm, we conducted several experiments on the SRR. A 3-axial gyroscope Crossbow VG400 is used to detect the roll angle and pitch angle of SRR. The parameters of the SRR is shown in Table.II. The joint velocity is limited within $3°/s$ to protect the manipulator.

TABLE II
PARAMETERS OF THE SRR

Parameter	Value	Parameter	Value
l_1	0.430 (m)	m_1	3.51 (kg)
l_2	0.395 (m)	m_2	3.02 (kg)
l_3	0.230 (m)	m_3	1 (kg)
q_1	$[-90, 90](^\circ)$	l_{offset}	0.12 (m)
q_2	$[-180, 180](^\circ)$	h_{offset}	0.13 (m)
q_3	$[-135, 135](^\circ)$	w_{offset}	0.06 (m)
m_b	27 (kg)	l_{mb}	0.36 (m)
h_{mb}	0.09 (m)	w_{mb}	0.26 (m)

A. Rollover avoidance

Four obstacles from low to high were placed in front of the SRR as shown in Fig.8. The SRR passed through these obstacles with its left track on the obstacles and right track on the floor. The initial configuration vector was set as $q = [-5^\circ, 5^\circ, 5^\circ]$. So, the initial system center of gravity was relatively high from the base platform, and the roll angle would have a great impact on the system rolling stability. The margin w_m was set at $0.06m$. The trajectories of the rolll and pitch are plotted on Fig.9. The SRR tracked on the highest obstacle about when $t = 17s$.

Fig. 8. Rollover avoidance experiment setup

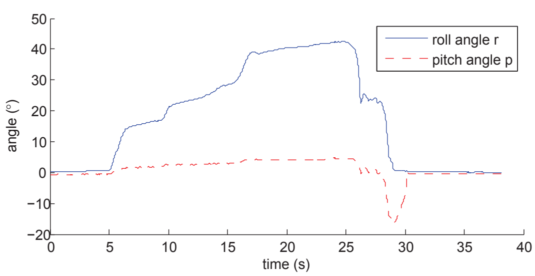

Fig. 9. Orientation data of SRR in experiment A

The safety state of SRR during obstacle crossing process is shown in Fig.10. The roll angle had an inverse proportional relationship with the limitation defined in Eq.7. And as the roll angle increased, the projection of SCG was moving away from origin in the Y_t-axis. SRR system entered into the rollover risk period (marked as period T in Fig.10 and Fig.11) at about $t = 19s$. The algorithm started updating the desired SCG for rollover avoidance by adjusting manipulator configuration at this stage. Fig.11 shows the manipulator joint angle trajectory. It also shows that the joints were adjusted and reached the desired angles in period T. For the rest of the time, the joints were adjusted according to secondary task. Fig.12 shows the SCG trajectory in $X_bO_bZ_b$ plane, and Fig.13 illustrates the manipulator posture over time. All the experimental results have proved that the algorithm had successfully prevented the SRR system from rolling over.

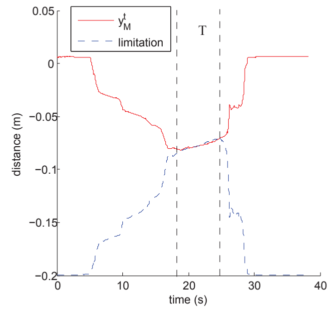

Fig. 10. Safety state of SRR in experiment A

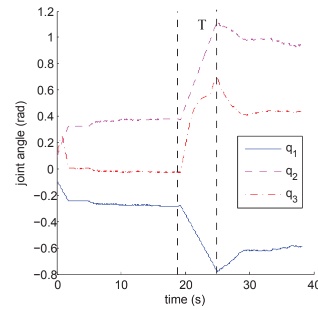

Fig. 11. Joint angle of manipulator in experiment A

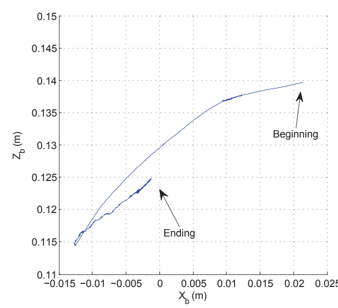

Fig. 12. Trajectory of SCG in experiment A

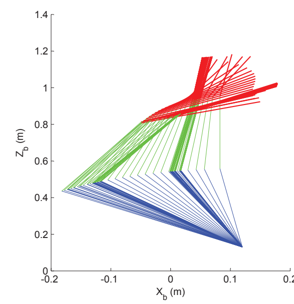

Fig. 13. Manipulator posture in experiment A

B. Tipover avoidance for SRR climbing stairs

In the stairs climbing experiment, the staircase size parameters are $h_{step} = 0.185m$, $h_{step} = 0.315m$ and $\theta_s \approx 30^\circ$. The initial configuration vector for manipulator was set as $q = [-80^\circ, 170^\circ, 0^\circ]$. Fig.14 presents the roll and pitch angle trajectory of SRR, Fig.15 shows the trajectory of the angle of the manipulator joint over time as it was climbing. The whole process is divided into four periods from $T1$ to $T4$ as shown in Fig. 14 and Fig. 15. Firstly, the SRR was climbing onto the stairs with the flipper. Eq.20 was not satisfied in period $T1$, so the manipulator control was predominately the secondary task functions. In $T2$ period, algorithm stoped the SRR and started to control the manipulator, so that the SCG was moved to the desired position. In $T3$ period, SRR was climbing on the nose line of stairs, and the SCG was maintained at the desired position. It can be seen from Fig.14 that the forward turning angle at the first stair was about 29°, which was consistent with the desired turning angle defined in Eq.14. When the SCG passed the last step and on the period $T4$, the secondary task functions resumed to control the manipulator.

The SCG trajectory in $X_bO_bZ_b$ plane and the manipulator posture are presented in Fig.16 and Fig.17 respectively. In

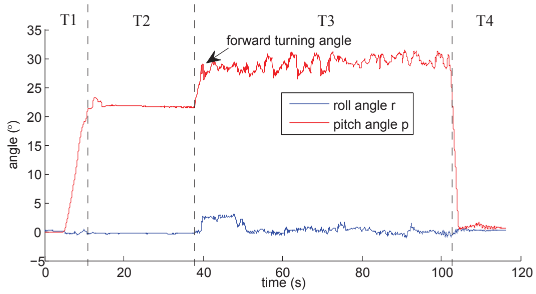

Fig. 14. Orientation data of SRR in experiment B

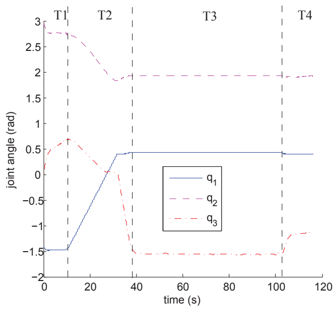

Fig. 15. Joint angle of manipulator in experiment B

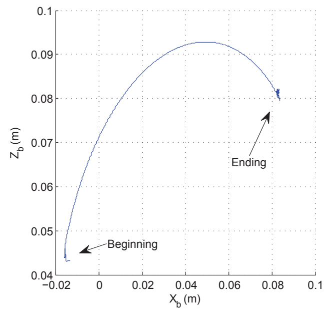

Fig. 16. Trajectory of SCG in experiment B

order to observe the optimization effect of the algorithm, the experiment was conducted again under the same circumstances, but this time the algorithm is not used. The two experimental results of the pitch angle in the period $T3$ are compared in Fig.18. It is clear that the 42° forward turning angle from the later experiment was much larger than the angle from the formal experiment. The vibration amplitude and average value of pitch angle are also much larger than the experimental results of the formal experiment. These results prove that the algorithm greatly improved the stability of the SRR.

VI. CONCLUSIONS

This paper presents an algorithm to stabilize the mobile manipulator by assessing and altering the position of the overall center of gravity. We implemented the algorithm onto a tracked search and rescue robot. The static equilibrium analysis provided us with the tipover criteria for the SRR. The velocity kinematics model of the onboard manipulator was built for the SCG adjustment. We set up the experiment for the SRR to cross over obstacles and stairs. The experimental results verified the functionality of our proposed algorithm. In future works, we will include the dynamics to improve the algorithm.

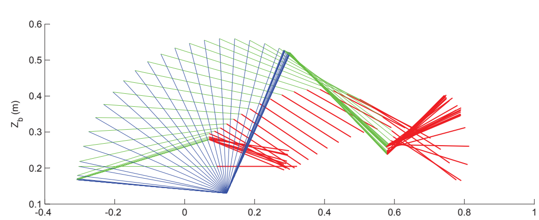

Fig. 17. Manipulator posture in experiment B

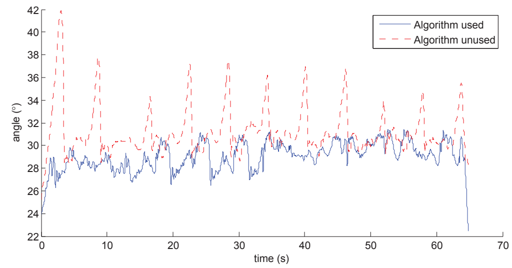

Fig. 18. Comparison of the pitch angle trajectory of SRR in stair climbing process

REFERENCES

[1] M. Raibert, K. Blankespoor, G. Nelson, R. Playter, *et al.*, “Bigdog, the rough-terrain quadruped robot,” in *Proceedings of the 17th World Congress*, 2008, pp. 10 823–10 825.

[2] E. Moore, D. Campbell, F. Grimminger, and M. Buehler, “Reliable stair climbing in the simple hexapod’rhex’,” in *IEEE International Conference on Robotics and Automation, ICRA.*, vol. 3, 2002, pp. 2222–2227.

[3] C.-K. Woo, H. D. Choi, S. Yoon, S. H. Kim, and Y. K. Kwak, “Optimal design of a new wheeled mobile robot based on a kinetic analysis of the stair climbing states,” *Journal of Intelligent and Robotic Systems*, vol. 29, no. 4, pp. 325–354, 2007.

[4] B. Yamauchi, “Packbot: A versatile platform for military robotics,” in *Proc. SPIE*, vol. 5422, 2004, p. 229.

[5] L. Matthies, Y. Xiong, R. Hogg, D. Zhu, A. Rankin, B. Kennedy, M. Hebert, R. Maclachlan, C. Won, T. Frost, *et al.*, “A portable, autonomous, urban reconnaissance robot,” *Robotics and Autonomous Systems*, vol. 40, no. 2, pp. 163–172, 2002.

[6] N. Mourikis, Anastasios I.and Trawny, S. I. Roumeliotis, D. M. Helmick, and L. Matthies, “Autonomous stair climbing for tracked vehicles,” *The International Journal of Robotics Research*, vol. 26, no. 7, pp. 737–758, 2007.

[7] Y. Xiong and L. Matthies, “Vision-guided autonomous stair climbing,” in *Proceedings of the 2000 IEEE International Conference on Robotics and Automation, ICRA.*, vol. 2, 2000, pp. 1842–1847.

[8] M. Mosadeghzad, N. D., and G. S., “Dynamic modeling and stability optimization of a redundant mobile robot using a genetic algorithm,” *Robotica*, vol. 30, pp. 505–514, 2011.

[9] A. Ghaffari, A. Meghdari, D. Naderi, and S. Eslami, “Enhancement of the tipover stability of mobile manipulators with non-holonomic constraints using an adaptive neuro-fuzzy-based controller,” *Proceedings of the Institution of Mechanical Engineers, Part I: Journal of Systems and Control Engineering*, vol. 223, no. 2, pp. 201–213, 2009.

[10] Y. Liu and G. Liu, “Trackstair interaction analysis and online tipover prediction for a self-reconfigurable tracked mobile robot climbing stairs,” *IEEE/ASME Transactions on Mechatronics*, vol. 14, no. 5, pp. 528–538, 2009.

[11] Y. Guo, A. Song, J. Bao, H. Zhang, and H. Tang, “Research on centroid position for stairs climbing stability of search and rescue robot,” *International Journal of Advanced Robotic Systems*, vol. 7, no. 4, p. 24, 2010.

[12] H. Zhang, Y. Jia, and N. Xi, “Sensor-based redundancy resolution for a nonholonomic mobile manipulator,” in *IEEE/RSJ International Conference on Intelligent Robots and Systems (IROS)*, Vilamoura,Portugal, Oct 2012, pp. 5327–5332.